NOAA NESDIS
CENTER FOR SATELLITE APPLICATIONS AND RESEARCH

GOES EVAPOTRASPIRATION (ET) AND DROUGHT PRODUCT SYSTEM (GET-D) ALGORITHM THEORETICAL BASIS DOCUMENT

Version 1.0

TITLE: GET-D ALGORITHM THEORETICAL BASIS DOCUMENT VERSION 1.0

AUTHORS:

Xiwu Zhan (NESDIS-STAR)

Christopher R. Hain (NESDIS-STAR/UMD-ESSIC-CICS)

Li Fang (NESDIS-STAR/UMD-ESSIC-CICS)

Zhengpeng Li (NESDIS-STAR/UMD-ESSIC-CICS)

GET-D ALGORITHM THEORETICAL BASIS DOCUMENT
VERSION HISTORY SUMMARY

Version	Description	Revised Sections	Date
1.0	New document adapted from STAR EPL guidelines for GET-D product system Critical Design Review (CDR)	New Document	9/15/2013
1.6	Revised for the GET-D Operational Readiness Review (ORR)	Table 1, Section 3.2.2, Table 6, Section 3.6.2	1/15/2016

TABLE OF CONTENTS

LIST OF FIGURES

Page

LIST OF TABLES

Page

LIST OF ACRONYMS

ABL	Atmospheric Boundary Layer
ALEXI	Atmosphere-Land Exchange Inversion model
ATBD	Algorithm Theoretical Basis Document
CDR	Critical Design Review
EF	Evaporative fraction
ESI	Evaporative stress index
ET	Evapotranspiration
GET-D	GOES ET and Drought Product System
CFS	Climate Forecast System
GOES	Geostationary Operational Environmental Satellites
LAI	Leaf area Index
LST	Land Surface Temperature
NARR	North American Regional Reanalysis
NCEP	National Center for Environmental Prediction
NLDAS	North America Land Data Assimilation System
PET	Potential ET
QC	Quality Control flags
SCAN	USDA Soil Climate Analysis Network
SMACEX	Soil Moisture-Atmospheric Coupling Experiment
SPI	Standardized Precipitation Index
TSEB	Two-Source Energy Balance Model
TSTIM	Two-Source Time-Integrated Model
UMD	University of Maryland
USDM	US Drought Monitor

ABSTRACT

NCEP needs independent ET data from satellite for validating Noah land surface model output and satellite based drought data product for monthly drought briefing. Under the request of SPSRB #0905-0007, "A GOES Thermal Observation Based Evapotranspiration (ET) Product", ET and drought producing system is designed to operationally generate hourly ET and drought maps at 12 km resolution based on GOES thermal observations.

The Atmosphere-Land Exchange Inversion model (ALEXI) is capable of computing principle surface energy fluxes, including ET, which is a critical boundary condition to weather and hydrologic modeling, and a quantity required for regional water resource management. ALEXI ET estimates have been rigorously evaluated in comparison with ground-based data, and perform well over a range in climatic and vegetation conditions. A simple evaporative stress index (ESI), which represents anomalies in remotely sensed ET/PET fraction generated with ALEXI flux estimates will be used as a drought monitoring tool. Anderson et al. (2007b; 2011) has demonstrated that ALEXI ESI over the continental US (CONUS) shows good correspondence with standard drought metrics and antecedent precipitation, but can be generated at significantly higher spatial resolution.

To meet the operational requirements, GOES ET and drought product system (GET-D) is designed to generate ET and drought maps operationally. ALEXI ET is retrieved over clear-sky pixels daily and ALEXI drought product is generated over 1 to 6 month compositing periods each day. Besides, ET and drought monitoring maps generated from GET-D are converted to the required formats (GRIB and others) and sent to STAR/OSPO for QC monitoring, to ESPC DDS server for distribution and to NCDC for archiving if needed. Satellite derived ET data are critical to improving land surface model simulations and the improvement of the numerical weather/climate forecasts. More accurate and complete ET and drought products are critical for global and US agricultural management and forecasts.

1. INTRODUCTION

Monitoring evapotranspiration (ET) and the extent and severity of agricultural drought is an important component of food and water security and world crop market assessment. Currently, no spatially distributed land surface ET product is available routinely from satellite observations. The existing MODIS ET product (called MOD16) is experimental and generated only by University of Montana for a few past time periods. GOES thermal observation based ET product is in high demand in National Center for Environmental Prediction (NCEP) for validating Noah land surface model output and satellite based drought data product for monthly drought briefing. Moreover, ET/drought information is greatly needed in USDA FAS/NASS/ARS for world crop forecasts and US agricultural production monitoring. A NESDIS funded GIMPAP project demonstrated that the Atmosphere-Land Exchange Inversion model (ALEXI) using GOES land surface temperature (LST) and solar insolation observations could produce reliable ET and drought data product routinely Anderson et al. 1997, 2007a,b, 2011). Since the GOES data are operationally available within NESDIS, generating ET and drought data products via the ALEXI model will meet the data needs by NCEP groups and other users. Under the circumstances, GOES ET and drought product system (GET-D) is designed to generate ET and drought maps operationally.

The ALEXI model is built on the two-source energy (TSEB) approach of Norman et al. (1995), which partitions the composite surface radiometric temperature acquired from a satellite-base platform, into characteristic soil and canopy temperatures, based on a fraction of vegetation cover (Anderson et al. 2005, Anderson et al. 1997, Mecikalski et al. 1999). For regional applications, the TSEB has been coupled with a 1-dimensional atmospheric boundary layer (ABL) model (McNaughton et al. 1986). In ALEXI, the lower boundary conditions for the two-source model are provided by TIR observations taken at two times during the morning hours from a geostationary platform such as GOES. The ABL model then relates the rise in air temperature above the canopy during this interval and the growth of the ABL to the time-integrated influx of sensible heating from the surface, and ET is computed as a partial residual to the energy budget. Use of time-differential measurements of surface radiometric

temperature reduces model sensitivity to errors in sensor calibration, and atmospheric and surface emissivity corrections (Kustas et al. 2001). The physical and mathematical description of ALEXI is given in the section 3.3 in detail.

ALEXI computes the principle surface energy fluxes, including ET, which is a critical boundary condition to weather and hydrologic modeling, and a quantity required for regional water resource management. ALEXI ET estimates have been rigorously evaluated in comparison with ground-based data, and perform well over a range in climatic and vegetation conditions. Evapotranspiration deficits in comparison with potential ET (PET) rates provide proxy information regarding soil moisture availability. In regions of dense vegetation, ET probes moisture conditions in the plant root zone, down to meter depths. A simple evaporative stress index (ESI), which represents anomalies in the ratio of actual-to-potential ET (f_{PET}), can be developed from ALEXI flux estimates. ESI has a value of 0 when there is ample moisture/no stress, and a value of 1 when evapotranspiration has been cut off because of stress induced stomatal closure and/or complete drying of the soil surface. Anderson et al. (2007b; 2011) has demonstrated that ALEXI ESI over the continental US (CONUS) shows good correspondence with standard drought metrics and antecedent precipitation, but can be generated at significantly higher spatial resolution due to a limited reliance on ground observations. As a diagnostic indicator of actual ET, accounting for both precipitation and non-precipitation related inputs to the plant-available soil moisture pool (e.g., irrigation, shallow groundwater), the ESI is a measure of actual vegetation stress rather than potential for stress. Because precipitation is not used in construction of the ESI, this index provides an independent assessment of drought conditions and will have particular utility for real-time monitoring in regions with sparse rainfall data or significant delays in meteorological reporting.

In summary, The ALEXI surface energy balance model was specifically designed to minimize the need for ancillary meteorological data while maintaining a physically realistic representation of land-atmosphere exchange over a wide range in vegetation cover conditions. These advantages make ALEXI capable of routine, long-term mapping of ET and soil moisture stress. The ET and drought monitoring products from GET-D will be validated against multi-source in situ ET observations and

various existing drought indices, e.g. US Drought Monitor, Standardized Precipitation Index (SPI), etc.

1.1. Purpose of This Document

This GET-D Algorithm Theoretical Basis Document (ATBD) explains the physical and mathematical background for algorithm to derive ET and drought maps based on land surface temperature (LST) and solar insolation observations from GOES Imagers and meteorological forcing from NCEP models in NLDAS. This document provides an overview of the required input data, the physical and mathematical descriptions of the retrieval algorithms, its predicted performance, sensitivity study of the algorithm, practical considerations, and assumptions and limitations.

1.2. Who Should Use This Document

The intended users of this document are those interested in understanding the physical bases of the ET and drought maps process algorithms and how to use the outputs of GOES ET and drought products for a particular application. This document also provides information useful to anyone maintaining or modifying the original algorithms.

1.3. Inside Each Section

This ATBD includes four sections:
Section 1.0 – Introduction, provides the purpose, intended users, and revision history of the ATBD.
Section 2.0 – System Overview, briefly describes the system architecture of the ET and drought product system, including system inputs, data flow and system outputs.
Section 3.0 - Algorithm Description, provides the algorithm details including a processing overview, input data, physical and mathematical description, algorithm output, performance estimates, practical considerations, and preliminary validation results.

Section 4.0 – Assumptions and Limitations, states assumptions presumed in determining that the software system architecture as designed will meet the requirements and states limitations that may impact on the system's ability to meet requirements.

Section 5.0 - List of References. gives a list of references cited in the document.

1.4. Revision History

The initial version (1.0) of this GET-D ATBD produced for the GET-D Critical Design Review (CDR) conducted on August 21, 2014.

This revised version 1.6 is prepared for the GET-D Operational Readiness Review (ORR) to be conducted on February 5, 2016.

2. SYSTEM OVERVIEW

This section gives the overview of the framework of the GOES ET and drought product system.

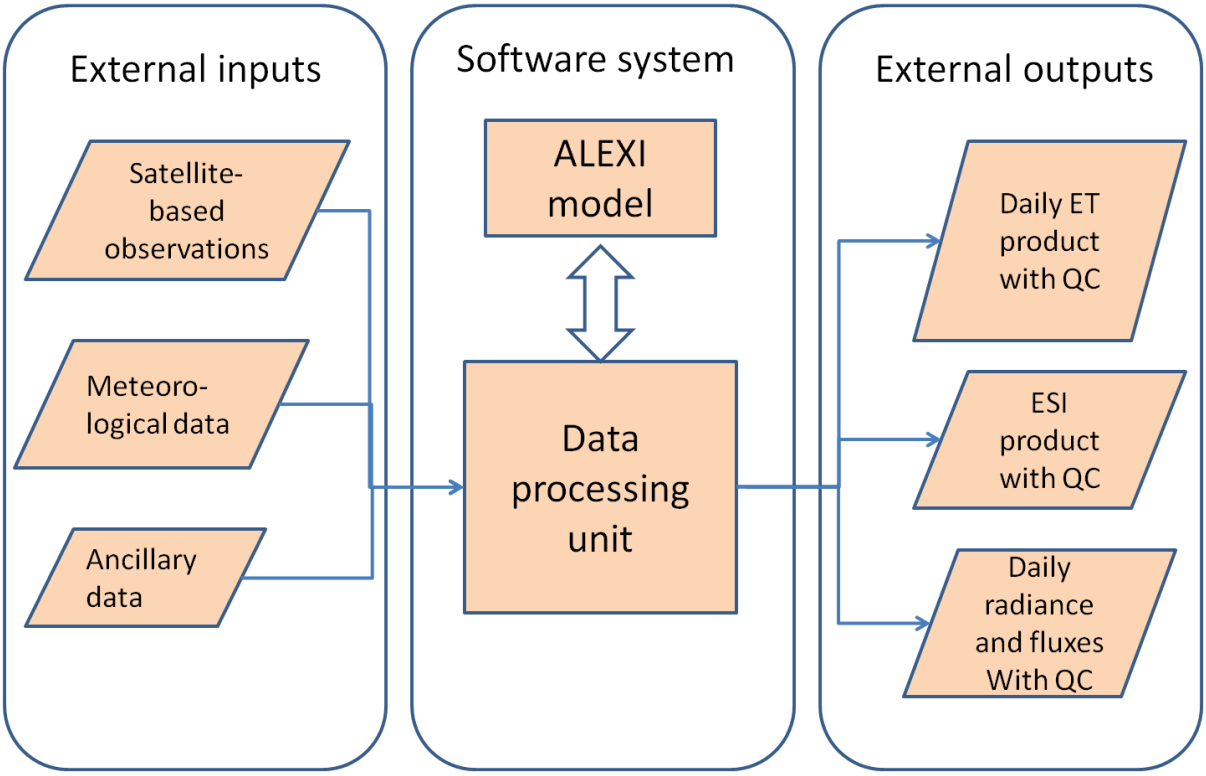

Figure 1 Overview of GET-D system design

2.1 Products Generated and product requirement

The GET-D system is capable of producing ET and drought maps which meet all the requirements in terms of accuracy, latency, resolution et al. Details are summarized in Table 1.

Table 1 GET-D system requirements

	Requirement	Proposed capabilities
Satellite sources	GOES-East and West	Same as requested
Accuracy	< 20%	Same as requested
Latency	24 hours	Same as requested
Timeliness	Hourly	Same as requested
Coverage	CONUS and North America	Same as requested
Resolution	8 km	Same as requested
Other attributes	Monthly composites are needed for climate assessment	Daily and monthly composites will be generated and validated

3. ALGORITHM DESCRIPTION

3.1 Processing Overview

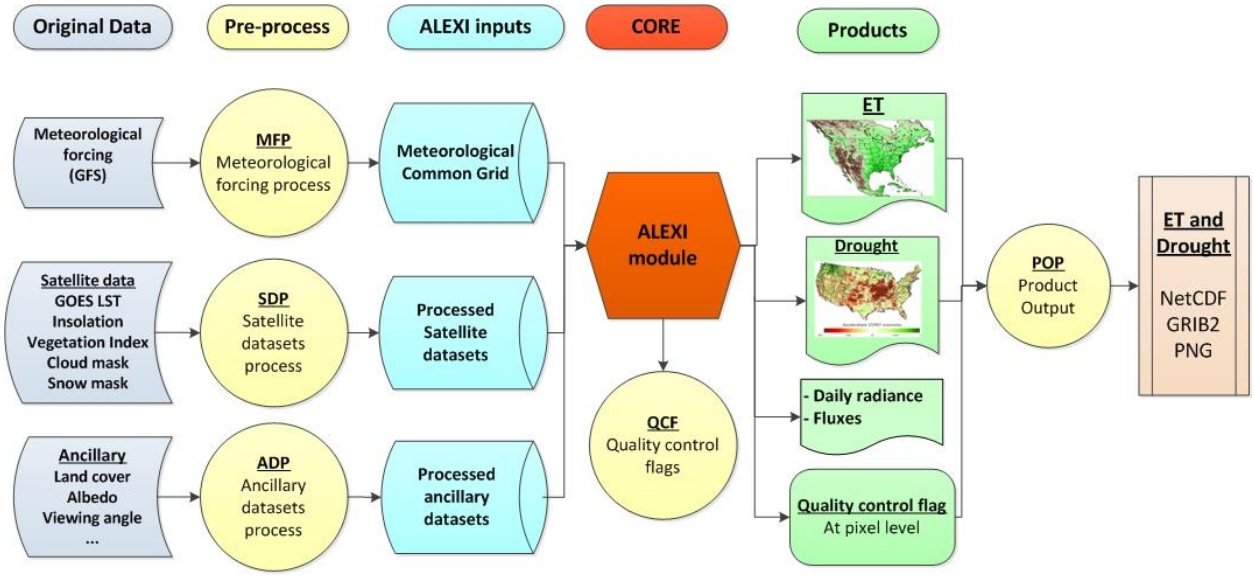

Figure 2 System design of GET-D

3.2 Algorithm Input

This section describes the input needed to process the GOES thermal-observation based ET and drought products. Satellite-based LST and solar insolation from GOES Imagers and meteorological forcing from NCEP models via NLDAS are two major inputs to the system. Besides, some ancillary data are also required in GET-D system, which will be introduced in this section as well.

3.2.1 Satellite-based Observations

Table 2 contains the primary sensor data used in GET-D system. The primary real time satellite-based inputs are GOES LST at 3.7 and 11 micron channel at 4 km spatial resolution, and incoming solar radiation from GSIP with the resolution of 0.125 degree. The leaf area index (LAI) is another crucial input to ALEXI. Moreover, solar and satellite geometry information is required as well. Sensor data, data sources, and their descriptions are given in detail in the table.

Table 2 List of input from primary sensor data

Name	Data Type	Resolution	Source & Description
GOES LST	float	4km	GOES East/West Imagery; 11micron/3.7 micron channel brightness temperature
Insolation	float	0.125 degree	ET: GSIP real time insolation; ESI: Climatological Clear-sky (static)
LAI	float	1 km	Primary Option: MODIS LAI (MOD15A2); Secondary Option: NESDIS GVF (inverted to LAI)
Latitude	float	4km	Pixel latitude
Longitude	float	4km	Pixel longitude
Solar zenith	float	4km	GOES solar zenith angles
View zenith	float	4km	GOES view zenith angle
QC Flags	int	Pixel resolution	GOES quality control flags

3.2.2 Meteorological Data

The GET-D system is designed to ingest meteorological data from multi-sources. The selection of meteorological data is controlled by the configuration file. The meteorological data is NCEP Climate Forecast System (CFS). The detailed description of these two meteorological dataset is listed in Table 3 and 4. Specific forcing variables extracted from the meteorological datasets can be divided into two categories, 2-D variables and 3-D variables, which are listed in Table 3. The original NARR meteorological data are in GRIB format and CFS in GRIB2, which will be converted to binary during the pre-process. The extracted variables with their corresponding ID in original formats are listed in Table 4.

Table 3 Spatial coverage and resolution of meteorological datasets (NARR & CFS)

	NARR	CFS
East Longtitude	-	180
West Longtitude	-	-180
North Latitude		90
South Latitude	0.9992	-90
Spatial Resolution	0.3 degree	0.5 degree
Temporal resolution	3 hour	6 hour
Projection	LambertConformal	GaussianCylindrical

Table 4 Description of extracted variables from meteorological data (NARR & CFS)

Variables	NARR	CFS - ID	Type
Temperature (1000mb to 100 mb)	TMP:100 mb- 1000 mb	TMP:100 mb - 1000 mb	3-D
Geopotential Height(1000mb to 100 mb)	HGT:100 mb - 1000 mb	HGT:100 mb - 1000 mb	3-D
RH/SPFH at Pressure (1000mb to 100 mb)	SPFH: 100 mb - 1000 mb	RH:100 mb - 1000 mb	3-D
Surface temperature	TMP:30 m above ground	TMP:80 m above ground	2-D
Surface pressure	PRESSURE: 30 m above surface	PRES: 80 m above ground	2-D

Surface specific humidity/relative humidity/mixing ratio	SPFH:30 m above ground	SPFH: 80 m above ground	2-D
Surface geopotential height	narr_sfc_height.dat	80 meter constant	2-D
Surface wind speed	UGRD:30 m above ground VGRD:30 m above ground	UGRD:80 m VGRD:80 m	2-D
Downwelling longwave radiation	DLWRF:sfc	Downward Long-Wave Rad. Flux*	2-D

*CFS only contains the Downward Long-Wave Rad. Flux in the forecast data, not in the analysis data.

Process of the input meteorological will be needed when the input meteorological variables are not used by the ALEXI model. As a example, we have Geopotential Height in the input from and will need to convert it into Geometric Height.

3.2.3 Ancillary Data

Ancillary data required for the GET-D system include cloud mask and land cover map.

Real time GSIP cloud mask will be adopted in the process of ET generation and internal two-channel threshold cloud mask will be used for ESI map generation.

ALEXI requires several variables that are used to describe the characteristics of the canopy and are subsequently used to calculate exchange coefficients between the atmosphere and canopy. The land-surface classification currently used in GET-D system is the University of Maryland (UMD) 1-km Global Land cover Product which consists of twelve vegetation classes. Figure 3 shows the spatial representation of the UMD land cover product across the continental United States.

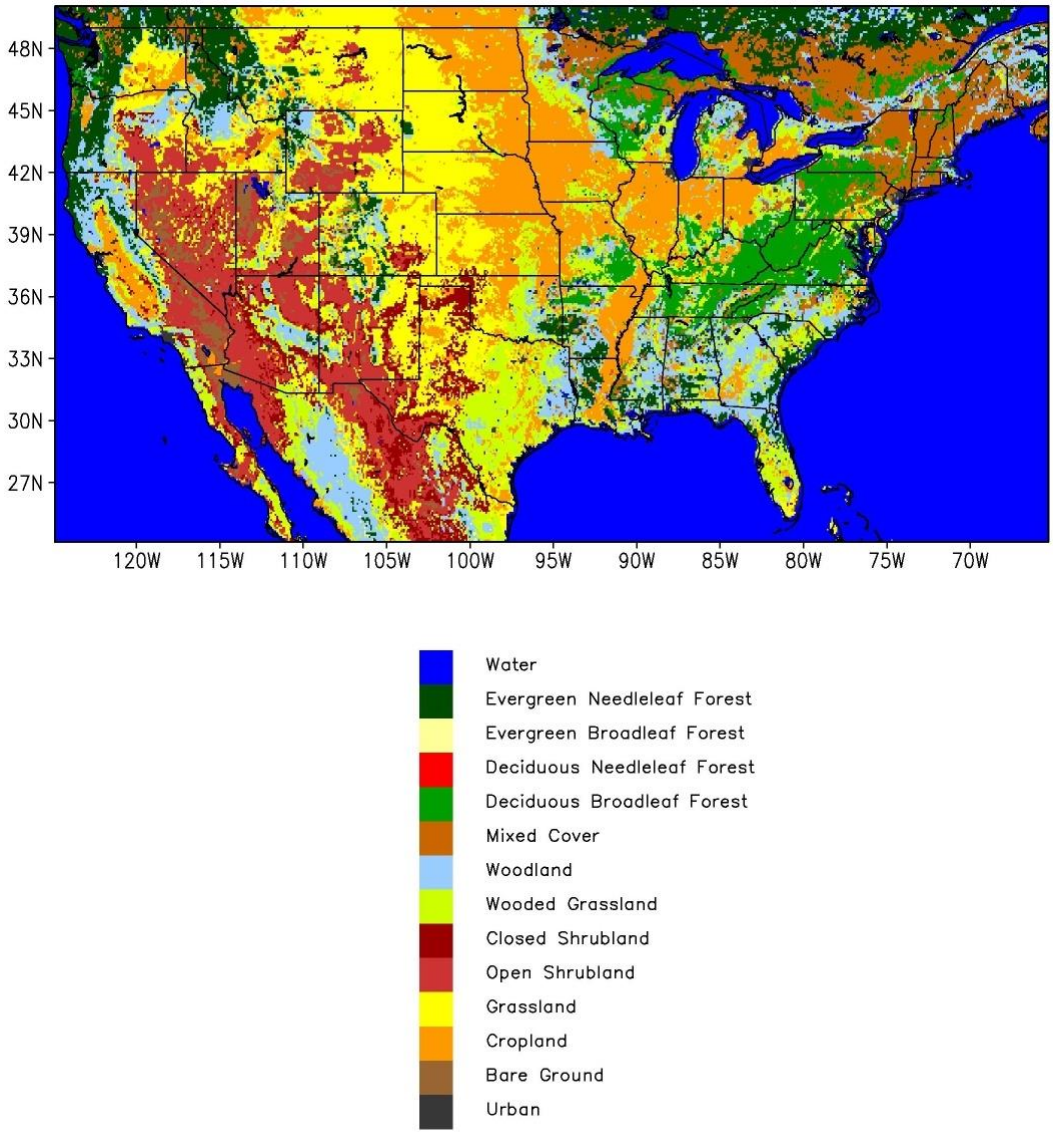

Figure 3 UMD Landcover Classification for the continental United States

3.3 Theoretical Description

3.3.1 ALEXI model

ALEXI model was originally called the Two-Source Time-Integrated Model (TSTIM), which was an extension of the Two-Source Energy Balance Model (TSEB) developed by Norman et al. (Norman et al. 1995). The TSM was initially developed to address many of the issues dealing with the monitoring of surface fluxes from satellite-based platforms (Anderson et al. 1997). The main issue addressed in the TSM formulation was the common misuse or misrepresentation of the radiometric surface temperature as the equivalent of the aerodynamic temperature of the surface (Anderson et al. 1997). This variable plays an important role in the calculation of heat transfer within the atmospheric surface layer.

The TSM estimates instantaneous heat fluxes given singular measurements of surface brightness temperature and air temperature. It has been found that two-source models represent advancement over single-layer models, which typically used the radiometric temperature to be representative of the aerodynamic temperature (Gash 1987, Hall et al. 1992, Jackson 1982). The single-layer approaches have been shown to overestimate sensible heat, especially over sparsely vegetated regions, because the resistance to heat transport from the soil component is often significantly larger than that from the vegetated component (Anderson et al. 1997). The relationship between the surface radiometric temperature and the aerodynamic temperature can be more accurately represented when the net surface flux is partitioned between the soil and canopy components (Anderson et al. 1997). Another significant upgrade with the two-source model is that the variation of surface radiometric temperature with sensor view angle can be predicted because the individual temperatures of both the soil and canopy are extracted from the composite temperature (Anderson et al. 1997).

The ALEXI model is made up of two atmospheric components, a surface-layer component and an atmospheric boundary layer component (Anderson et al. 1997). Figure 4 shows a schematic representation of both the surface and atmospheric boundary layer component of ALEXI. The implementation of an atmospheric boundary layer component was motivated by documented

relationships between the rise in temperature and height of the mixed layer to the time-integrated influx of sensible heating from the surface (Diak 1990, Culf 1993, Diak et al. 1995, Mecikalski et al. 1999, Tennekes 1973).

Flux partitioning in the ALEXI model is guided by time changes in surface brightness temperature, where the amplitude of the diurnal surface temperature wave has been found to be a good indicator of surface flux partitioning; wetter surfaces warm more slowly and expend more energy in evaporation (Idso et al. 1975, Diak 1990, Mecikalski et al. 1999, Wetzel et al. 1984). The use of a time-differential temperature signal reduces the impact of errors in sensor-based calibration errors, atmospheric corrections and assumed surface emissivity (Mecikalski et al. 1999, Anderson et al. 1997). This represents a significant upgrade over models that use observations of absolute temperature in their computations.

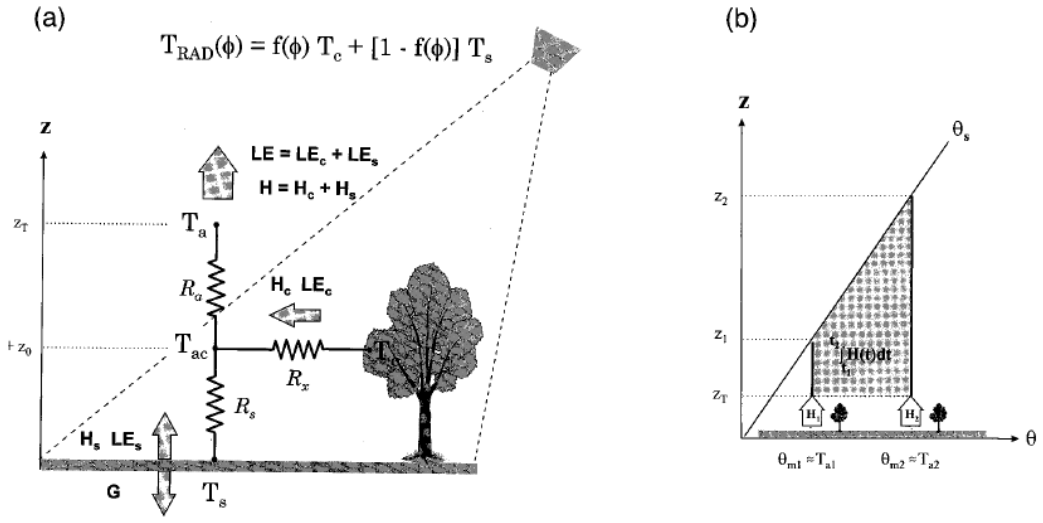

Figure 4 (a) A schematic description of the surface-layer component of ALEXI, and (b) the surface-layer model component is applied at times t_1 and t_2 during the morning hours, returning instantaneous sensible heat flux estimates. The time-integrated sensible heat flux during this interval serves to heat and grow the atmospheric boundary layer. Taken from Mecikalski et al. (1999).

The radiometric temperature of a vegetated surface is the ensemble average of the individual thermodynamic temperature of the soil (Ts), and the vegetation (Tc), weighted by their contribution to the brightness temperature:

$$T_{RAD}(\varphi) \approx \{ f(\varphi) T_c + [1 - f(\varphi)] T_s \}, \tag{3.1}$$

where f(φ) is the fraction of the sensor view angle occupied by vegetation when viewed at an angle φ from nadir (Norman et al., 1995). For a canopy with a random distribution of leaves, a spherical distribution of leaf angles, and a leaf area index F,

$$f(\varphi) = 1 - \exp\left(\frac{-0.5F}{\cos\phi} \right). \tag{3.2}$$

The net balance of energy at the earth's surface can be represented by

$$R_n = H + LE + G, \tag{3.3}$$

where Rn is the net radiation above the vegetated surface, and H, LE, and G are the net fluxes of sensible, latent and ground conduction heating, respectively. The surface layer component of ALEXI is computed using the following set of equations:

Soil and canopy energy budgets:

$$R_{n,s} = H_s + LE_s + G \tag{3.4a}$$

$$R_{n,c} = H_c + LE_c \tag{3.4b}$$

Net radiation:

$$R_n = R_{n,s} + R_{n,c} \tag{3.5a}$$

$$R_n = (L_d - L_u) + (S_d - S_u) \quad (3.5b)$$

$$R_n = L_d - (1-\tau_c)L_c - \tau_c L_s + (1-A)S_d \quad (3.5c)$$

$$R_{n,s} = \tau_c L_d + (1-\tau_c)L_c - L_s + (1-\rho_s)S_{d,s} \quad (3.5d)$$

Sensible heat:

$$H = H_s + H_c = \rho c_p \frac{T_{ac} - T_a}{R_a} \quad (3.6a)$$

$$H_s = \rho c_p \frac{T_s - T_{ac}}{R_s} \quad (3.6b)$$

$$H_c = \rho c_p \frac{T_c - T_{ac}}{R_x} \quad (3.6c)$$

Latent heat:

$$LE = LE_s + LE_c \quad (3.7a)$$

$$LE_c = \alpha_{PT} f_g \frac{\Delta}{\Delta + \gamma} R_{n,c} \quad (3.7b)$$

Ground heat:

$$G = 0.3R_{n,s}. \quad (3.8)$$

In the above equations, T is temperature, e is vapor pressure, R is an exchange resistance coefficient, ρ is air density, cp is the heat capacity of air at constant pressure, γ is the psychometric constant, and S is the slope of saturation vapor pressure versus temperature curve. The subscripts ‘a’, ‘ac’, and ‘x’ represent properties of the air above and within the canopy, and within the leaf boundary layer, respectively, while ‘s’ and ‘c’ represent the soil and canopy components of the system. The ground

heat flux is parameterized and computed using an expression developed by Choudhury (Choudhury et al. 1987), which computes the term as thirty percent of the net radiation available to the soil component of the system. Equation 3.7b is solved initially by a Priestly-Taylor approximation (Priestley et al. 1972). This approximation assumes that the canopy is transpiring at its maximum potential rate, an assumption that is often valid in regions where there is adequate water supply, but can tend to overestimate canopy transpiration in drier regions (Anderson et al. 1997).

Using brightness temperature measurements at times t1 and t2, and initial estimates of near-surface temperature, the surface component of ALEXI yields instantaneous sensible heat flux estimates, H_1 and H_2 (Anderson et al. 1997). Assuming a linear rise in sensible heat during the morning hours, which has been found to be valid when advection is negligible, a time-integrated heat flux can be computed by

$$\int_{t_1}^{t_2} H(t)dt = \frac{1}{2}(H_2 t_2 - H_1 t_1). \tag{3.9}$$

The ABL component of ALEXI is a simple slab model which describes the dynamics of the atmospheric boundary layer and is used as a closure technique to evaluate the morning evolution of air temperature, Ta, in the surface layer. It is assumed that all the air within the mixed layer is at a uniform potential temperature, and this value is related to the surface air temperature by

$$\theta_m = T_a \left(\frac{100}{p} \right)^{\frac{R}{c_p}}, \tag{3.10}$$

where *p* is the atmospheric pressure (in kPa) at the surface and R/cp = 0.286(Anderson et al. 1997). Tennekes (Tennekes 1973) showed that the height of the convective boundary layer at any time is uniquely defined by the current surface air temperature [through Equation (3.10)] and a morning temperature sounding. McNaughton and Spriggs (McNaughton and Spriggs 1986) presented a simplified conservation equation describing the growth of a convective boundary layer over time, assuming no subsidence and horizontal advection:

$$\int_{t_1}^{t_2} H(t)dt = \rho c_p (z_2\theta_{m_2} - z_1\theta_{m_1}) - \rho c_p \int_{z_1}^{z_2} \theta_s(z)dz, \qquad (3.11)$$

where $\theta_{m,1}$ is the potential temperature within the mixed layer and $\theta_s(z)$ is the potential temperature profile above the mixed layer at time t_1. The time-integrated sensible heat flux from the ABL component of ALEXI is computed given a value of $\theta_{m,2}$. Because differential surface temperature measurements are more reliable than absolute temperature measurements, in practice z_1 is fixed at some small value (~50 meters), and the change in modeled θ_m is allowed to govern the growth of the boundary layer based on the lapse rate profile above the mixed layer height, z_1 (Anderson et al. 1997). The sensible heat flux estimates from both the surface and ABL components of ALEXI are iterated until the time-integrated sensible heat flux estimates from both components converge (Anderson et al. 1997). Based on the computation of sensible heat flux for both the soil (H_s) and the canopy (H_c), the canopy transpiration (LE_c), the ground heat flux (G), and net radiation (R_n), the value for direct soil evaporation (LE_s) is solved as a residual to the surface energy budget calculation. Under drier conditions this can result in a direct soil evaporation of less than zero, which in unlikely during the midday period. This condition implies that the earlier assumption of the canopy transpiring at its potential rate is invalid, and in this case the canopy transpiration term is scaled back until the direct soil evaporation term is zero (Anderson et al. 1997).

A number of primary data sources are needed for the regional implementation of ALEXI and these data sources are summarized in Table 5.

Table 5 Input data sources for ALEXI on a regional scale

Data	Purpose	Source	Resolution (Spatial/temporal)
Clear sky:			
LST	Surface temperature change	GOES Imagery	4km/1hr
LAI	TSEB partitioning; assign hc, d, z0, esfc	MODIS	1km/8dy
Landcover type	Assign hc, d, z0, α, s,	UMD global	1km/fixed
SWDNi, LWDNi	Net radiation	GOES	12km/1hr
Wind	Transport resistances	ASOS/AWOS	40km/1hr
Dtheta/dz	ABL growth model	Radisonde	40km/3hr
T(z), q(z)	Atmospheric correction	Radiosonde	40km
Cloud amount	Cloud mask	GOES	12/1hr
Cloudy sky :			
Soil texture (0-5cm, 5-200cm)	Assign AWC	STATSGO	1km/fixed

3.3.2 Extrapolation from instantaneous to hourly and daily Fluxes

A common technique for extrapolating instantaneous satellite-based flux estimates to daily totals is to assume that the evaporative fraction (EF), given by the ratio of latent heat to the available energy, is constant during daylight hours for a given day (Gurney et al. 1990, Shuttleworth et al. 1989, Sugita et al. 1991). Given the value of EF determined at the ALEXI modeling time (t_2) along with hourly estimates of RN and G at times t_i, which can be obtained from GOES, hourly values of system sensible and latent heating can be computed for days with clear mornings as:

$$\lambda E_i = EF(RN_i - G_i)$$

$$H_i = RN_i - G_i - \lambda E_i$$

Previous studies have shown that daily total fluxes estimated using the EF measured at midday underestimate observed totals by 5 – 10% (Brutsaert et al. 1992, Gurney and Hsu 1990, Sugita and Brutsaert 1991, Zhang et al. 1995, Crago 1996), therefore EF is defined here as:

$$EF = 1.1\frac{\lambda E_2}{RN_2 - G_2}$$

using flux components computed at modeling time t_2.

For clear pixels, hourly fluxes from the soil component of the two-source system are obtained as:

$$EF_S = 1.1\frac{\lambda E_{S2}}{RN_{S2} - G_2}$$
$$\lambda E_{Si} = EF_S(RN_{Si} - G_i)$$
$$H_{Si} = RN_{Si} - G_i - \lambda E_{Si}$$

while the canopy components are determined as residuals:

$$\lambda E_{Ci} = \lambda E_i - \lambda E_{Si}$$
$$H_{Ci} = H_i - H_{Si}$$

Hourly E_{ci} and E_{si} are integrated to provide the daily total water extractions $\langle E_C \rangle$ and $\langle E_S \rangle$ used to update the root-zone and soil surface moisture pools (equation 7).

For cloudy pixels, hourly values of latent heat flux are simply estimated from hourly PET_i and contemporaneous stress function values, while sensible heat is computed as a residual to the component energy budget:

$$E_{Ci} = f_{PET_C} * PET_{Ci}$$
$$E_{Si} = f_{PET_S} * PET_{Si}$$
$$H_{Ci} = RN_{Ci} - E_{Ci}$$
$$H_{Si} = RN_{Si} - E_{Si} - G_i$$

3.3.3 Potential Evapotraspiration

The ratio of actual and potential ET requires the computation of a value for potential ET. Potential ET is the amount of ET that would occur under optimal conditions over a surface that is at or above field capacity. There are several documented methods that can estimate the value of PET; some are more complicated such as the Penman-Monteith method, while others such as the Priestley-Taylor approximation are much simpler. The Priestley-Taylor method was chosen to be used within the ALEXI modeling framework because of its relative simplicity and its need for a minimum amount of ancillary data sources. The computation of PET is handled separately between the vegetated and bare soil components of each ALEXI grid cell, and this is done by the partitioning of two equations with respect to the fraction of vegetation cover. Potential canopy transpiration using the Priestley-Taylor approximation can be computed by

$$PET_c = \alpha_c f_g \frac{S}{S+\gamma} RN_c. \tag{5.3}$$

Potential soil evaporation is also estimated with a modified Priestley-Taylor approximation documented by Tanner and Jury (1976).

$$\tau = \exp\left[\frac{-0.45 f_c}{\sqrt{2\cos\varphi_s}}\right] \tag{5.4}$$

$$PET_s = \alpha_s \frac{S}{S+\gamma} RN_s, \tag{5.5}$$

where τ is the canopy transmission factor, γ is the psychometric constant (0.067 kPa/°C), S is the differential of the saturation vapor pressure vs. temperature curve, φ_s is the solar zenith angle, f_c is the fraction of vegetation cover and R_n is the net radiation for both soil and canopy components. The value of α_c is held constant at 1.3, but the value of α_s is a function of the following expressions with a critical

value, τ_{crit} equal to 1.5, when τ is less than the critical value α_s is equal to 1. If τ is greater than the critical value, then α_s can be computed by

$$\alpha_s = \alpha_P - \left[\frac{(\alpha_P - 1)(1-\tau)}{(1-\tau_{crit})} \right], \tag{5.6}$$

where α_p is a potential value and is equal to 1.3.

Although ALEXI estimates the contribution of direct soil evaporation and canopy transpiration separately, partitioned by the percent of vegetation cover, in this study we use only the system (direct soil evaporation + canopy transpiration) actual and potential ET estimates. At present, the system f_{PET} from ALEXI appears to be more robust than do the components f_{PET} values, perhaps reflecting errors in the model partitioning of fluxes between the soil and canopy. Qualitative analyses show a large degree of noise in the direct soil evaporation fields, while the canopy transpiration fields tend to exhibit little variability. The total system (direct soil evaporation + canopy transpiration) estimates exhibit far less noise and in essence represent an estimate of a fraction of actual to potential ET. It appears that there is no degradation in quality when using the total system ET fields when comparing the two separate fields of direct soil evaporation and canopy transpiration. The contribution of canopy transpiration compared to that of direct soil evaporation is heavily dependent on several variables: the percent of vegetation cover, vegetation type, and days since the last rainfall. It has been observed that the first few centimeters of the soil profile can dry very quickly after rainfall. Its hydraulic conductivity with the root-zone is significantly reduced and the two layers become decoupled, and direct soil evaporation ceases (Anderson et al., 2005). The time scale of drying with the root-zone is substantially longer than that of the surface layer and plants can continue to transpire at significant rates even through long stretches with a lack of rainfall. The surface layer only represents a small percentage of available water in the soil profile, and even under relatively low percents of vegetation cover, plant transpiration is important and most likely is the dominant source of ET. The total system fraction of actual to potential ET can be expressed as

$$f_{PET_{System}} = \frac{LH_s + LH_c}{PET_s + PET_c}, \tag{5.7}$$

where the s and c subscripts represent the contributions from soil evaporation and canopy transpiration, respectively.

Under the assumption that available water within the surface and root-zone layers is responsible for the partitioning of LE and H, a percent of available water can be retrieved for the complete soil profile in an integrated sense, from a value of f_{PET} computed from ALEXI flux estimates and an estimate of potential ET. The scale of the complete integrated soil profile can be described as the depth at which roots extend to provide water to the vegetation. This depth varies as a function of vegetation type, and usually extends in a range of 1 to 2 meters but can extend down to several meters below the surface in extensive forest regions. The combination of the two separate ALEXI LH estimates is advantageous because it eliminates any error associated with aforementioned assumptions. It can be considered a disadvantage because while it solves for an integrated f_{AW} in the soil profile, it provides no information on the vertical distribution of available water. A wide range of relationships between f_{PET} and f_{AW} can be found in the literature, while the common similarities between each of the relationships is $f_{PET}=1$ at $f_{AW}=1$, and $f_{PET}=0$ at $f_{AW}=0$, a large degree of difference is found between these two endpoints (Anderson et al., 2005).

3.3.4 Evaporative stress index

Spatial and temporal variations in instantaneous ET at the continental scale are primarily due to variability in moisture availability (antecedent precipitation), radiative forcing (cloud cover, sun angle), vegetation amount, and local atmospheric conditions such as air temperature, wind speed and vapor pressure deficit. Potential ET describes the evaporation rate expected when soil moisture is non-limiting, ideally capturing response to all other forcing variables. To isolate effects due to spatially varying soil moisture availability, a simple evaporative stress index (ESI) can be developed from model flux estimates, given by 1 minus the ratio of actual to potential ET following the formulation of the CWSI and WDI. Using ALEXI, we can derive evaporative stress indices associated with the canopy (ESI_c), the soil surface (ESI_s), and the combined plant-soil system (ESI):

$$ESI_C = 1 - f_{PET_C} = 1 - \frac{E_C}{PET_C}$$
$$ESI_S = 1 - f_{PET_S} = 1 - \frac{E_S}{PET_S}$$
$$ESI = 1 - f_{PET} = 1 - \frac{E}{PET} = 1 - \frac{E_C + E_S}{PET_C + PET_S}$$

where EC, ES and E are the modeled actual ET fluxes (mm) from the canopy, soil and system, respectively, and PET_C, PET_S, PET are potential rates associated with these components (mm). These indices have a value of 0 when there is ample moisture/no stress, and a value of 1 when evapotranspiration has been cut off because of stress induced stomatal closure and/or complete drying of the soil surface.

3.4 Algorithm Output

Output of the GET-D systems mainly contains two data arrays: the LST values and associated quality control flags, which are described in Table 6. Evapotraspiration and drought maps for CONUS are the main outputs of the GET-D system, which will be generated at 12 km spatial resolution and daily temporal resolution. The ET and drought maps will be output in GRIB2 and NetCDF for analysis purpose and in PNG for quick monitoring purpose.

Along with the ET and drought maps, quality control flags (QC) will be generated at pixel level for the outputs in GRIB2 and NetCDF formats. The design for QC is described in detail in Table 7.

Table 6 System output data

Name	Satellite/sensor	Data type	resolution	Format
Evapotranspiration	GOES-East and West / Imagers	Int scaled	8 km/daily	GRIB2, NetCDF, PNG
Drought Map	GOES-East and West / Imagers	Int scaled	8 km/daily	GRIB2, NetCDF, PNG

Quality Control flags	Output	Byte	--	--

Table 7 Detailed descriptions about the design of quality control flags at pixel level

Byte	Bit	Flag	Source	Effect
1	0-1	GOES Data Availability	GOES QC flags	00=normal, 10=bad data, 11=missing data
	2-3	Surface Type	Land cover	00=land, 01=snow/ice, 10=in-land water, 11=sea
	4-5	Cloud	Cloud Mask	00=clear, 01=probably clear, 10=probably cloudy, 11=cloudy
	6	Snow	Snow fraction/mask	0=snow free (mean snow fraction < 0.2), 1=snow contamination (mean snow fraction >=0.2)
	7	Empty		Reserved for future use
2	0-1	Empty		Reserved for future use
	2	View Angle	Sensor zenith	0=normal, 1=large view angle (LZA>55 deg)
	3	Atmospheric Condition	TPW	00=dry atmosphere (wv<=2.0g/cm^2); 01=moist atmosphere(wv>2.0g/cm^2); 10= very moist(wv>5.0/cm^2)
	4-5	ET Quality	ET	00=high quality, 01= moderate quality, 11=poor quality
	6-7	Drought Quality	Drought map	00=high quality, 01= moderate quality, 11=poor quality

3.5 Validation

3.5.1 Validation plan

The validation of ALEXI flux estimates and ESI will be presented in this section to assess the ability of the model to perform a proper retrieval of any soil moisture or available water quantity. The validation plan will include the following aspects:

1. Ground ET measurements are obtained from AmeriFlux sites in US and used to evaluate ALEXI ET estimates.
2. ALEXI ET product is compared with output from the NLDAS system by NCEP-EMC.
3. Drought monitoring maps are compared with various existing drought indices, e.g. US Drought Monitor, Standardized Precipitation Index (SPI), etc.

(The proposal mentioned the ALEXI SM validation as "Soil moisture proxies converted from ET are compared with soil moisture measurements of USCRN, SCAN and USDA-ARS networks." I am wondering if it is necessary to validate SM proxies from ALEXI since the title of this project is ALEXI ET and Drought maps. Please advice, if necessary, I will add SM validation results in.)

3.5.2 Validation results

3.5.2.1 Validation of ALEXI surface flux estimates

ALEXI model has demonstrated satisfactory reliability of its ET estimates for test data sets (Anderson et al. 2007). Figure 5 shows 'monthly' (28-day) composites of clear-sky instantaneous latent heat flux from ALEXI at time t_2 (5.5 hours past local sunrise) for April – September of 2002 – 2004. Monthly composites of daytime total fluxes (including both clear and cloudy intervals) exhibit similar spatial characteristics.

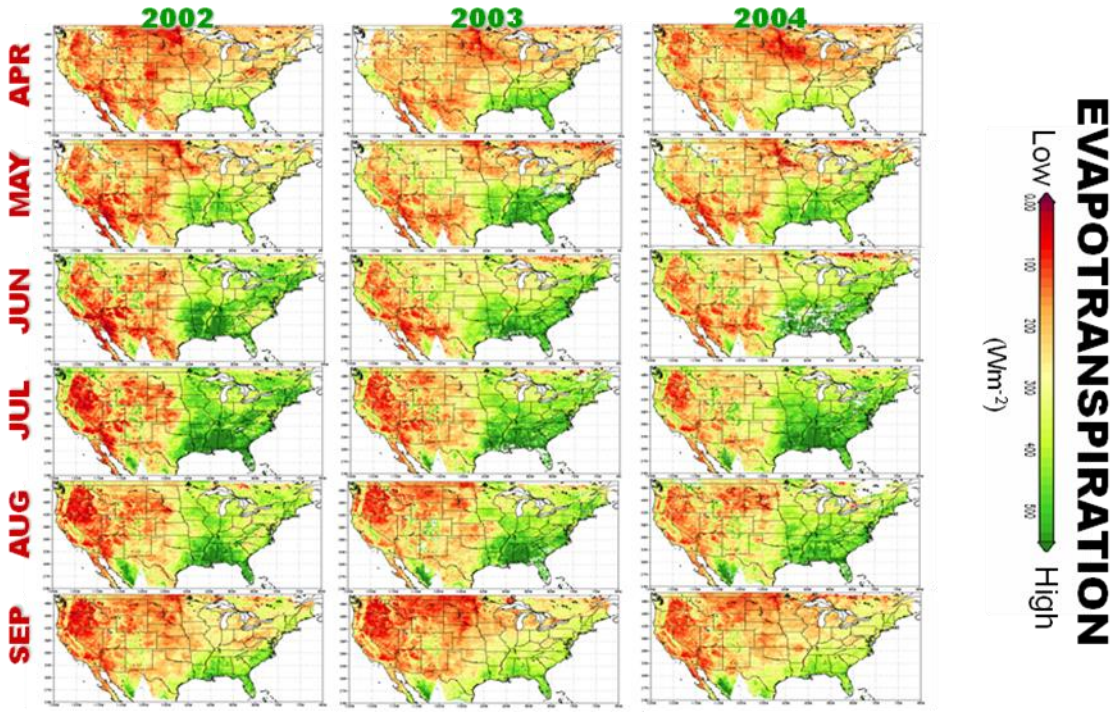

Figure 5 The 28-day clear-sky composites of instantaneous latent heat flux at time t2 for April – September of 2002 – 2004

Since ALEXI operates on a regional scale, it is unfortunately difficult to validate for several reasons. ALEXI executes on a spatial resolution of 8 km, which is a gross mismatch in scales when compared to the footprint of surface flux observations occurring on a scale of 0.1 to 1 km (Anderson et al. 2004). This limitation is further exacerbated over heterogeneous land cover pixels, where one surface flux tower location may not have vegetation properties that are representative of the complete 8 km pixel. Improved estimates of mean surface fluxes sampled at multiple locations within a pixel would provide better estimates for validation but require more financial and temporal resources (Doran et al. 1998, Gao et al. 1998). Anderson et al. (2004) implemented a technique to disaggregate regional surface fluxes to the micrometeorological scale, building on a technique initially developed by Norman et al. (Norman 2003). Disaggregation provides a possible solution to the limitations of the scale mismatch and addresses both the physical gaps encountered in upscaling ground observations to regional scales

and downscaling regional flux estimates to the footprint of a ground-based observation (Anderson et al., 2004).

The resulting high-resolution flux estimates may then be reaggregated and compared directly with tower observations, where some weighting function are used which describe the heterogeneity of the flux tower footprint (Anderson et al., 2004). The algorithm is valid under the assumption that horizontal fluxes are small in comparison with vertical fluxes and that conditions at 50 m AGL are more or less uniform on the spatial resolution of 5 km (Wieringa 1986, Mason 1988).

Although it is difficult to validate ALEXI surface fluxes, several large-scale field studies have implemented the necessary tools to measure surface fluxes, through eddy-covariance methods both at the ground and on aircraft. The most recent ALEXI surface flux validation occurred during the Soil Moisture-Atmospheric Coupling Experiment (SMACEX) which took place during the summer months of 2002 in the state of Iowa. Flux comparisons for both ALEXI and DisALEXI have been corrected for flux closure using the constant Bowen ratio method. RMSD from the validation exercises of SMACEX is 49 Wm-2 (Figure 6). Special care was taken during SMACEX to place flux towers equally between corn and soybean fields (dominant vegetation of the region), and when the modeled and measured fluxes are averaged over the complete domain, RMSD values improve to 25 Wm-2 (Anderson et al., 2007). DisALEXI flux estimates decrease the RMSE to value of 28 Wm-2 (Figure 7). The improved statistic provides a better estimate of the intrinsic model error of ALEXI, while showing that disaggregation is a very powerful validation tool, and can accommodate non-representative measurement sites, which provide a substantial degree of the observed error of ALEXI at both the 5-km and 10-km scale (Anderson et al., 2007).

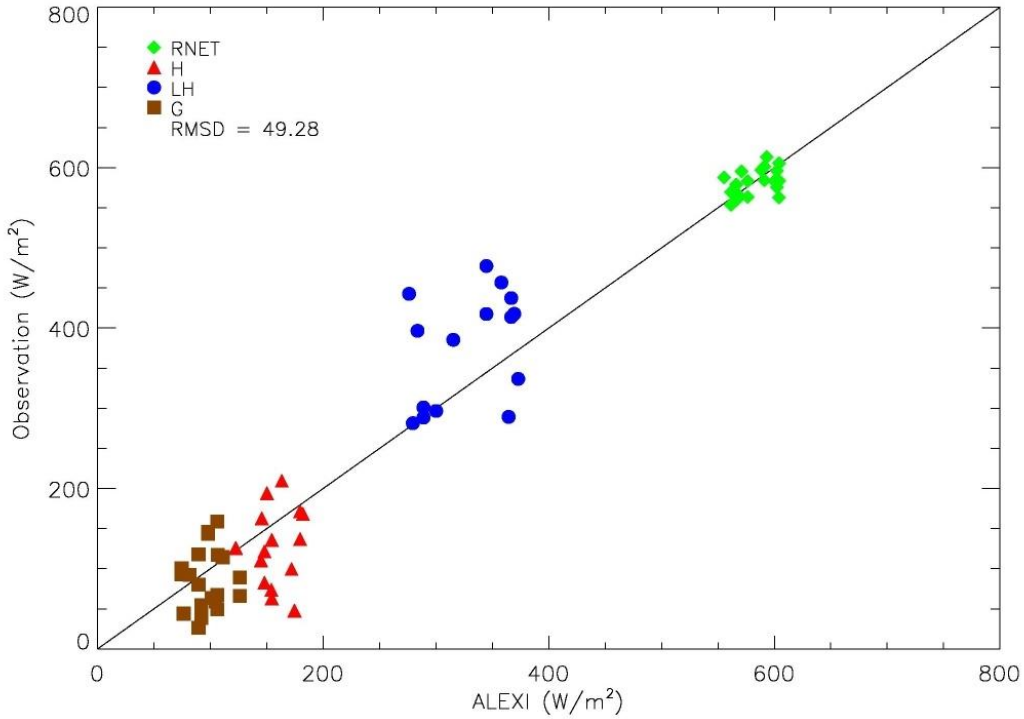

Figure 6 Scatter plot comparing ALEXI surface flux estimates with surface flux observations taken during the Soil Moisture Experiment (Iowa) in 2002. Surface fluxes and the RMSD value are expressed in Wm^{-2}. Taken from Anderson et al. (2007).

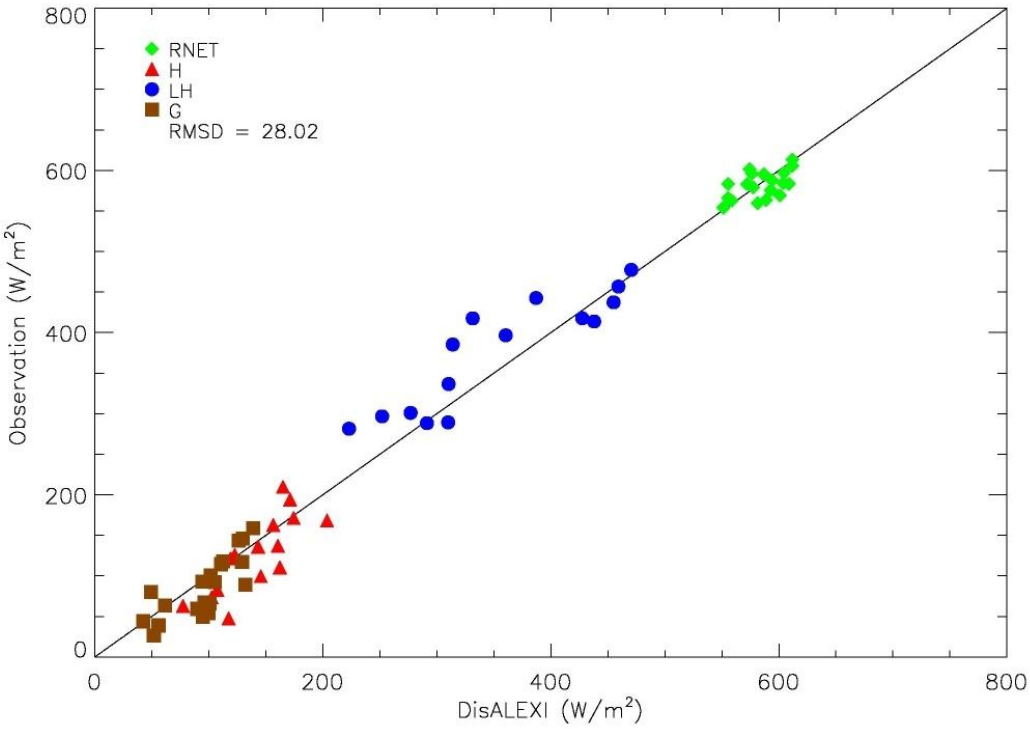

Figure 7 Scatter plot comparing ALEXI surface flux estimates with surface flux observations taken during the Soil Moisture Experiment (Iowa) in 2002. Surface fluxes and the RMSD value are expressed in Wm^{-2}. Taken from Anderson et al. (2007).

3.5.2.2 Validation of drought monitoring maps (ESI)

The drought monitoring maps (ESI) are compared with existing drought indices, such as US Drought Monitor (USDM) and Standardized Precipitation Index (SPI). An extensive index intercomparison study over the U.S. for 2000-2009 demonstrated that the ESI shows good correspondence with standard meteorological drought indices and with drought classifications recorded in the USDM (Figure 8; Anderson, et al., 2007c, 2010a). Unique behavior is observed in the ESI where non-precipitation moisture inputs are likely to be important, serving to temper local drought impacts.

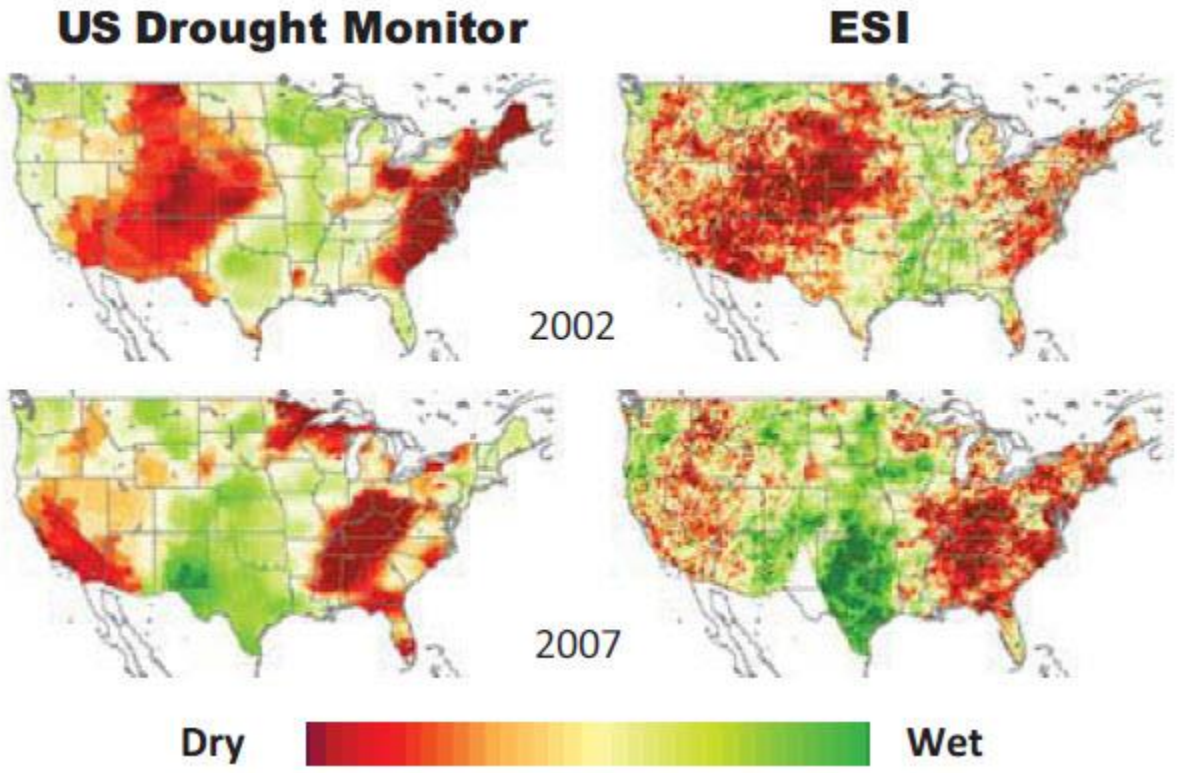

Figure 8 Comparison of seasonal (April-Sept.) anomalies in USDM drought classifications and the ALEXI ESI product for two major drought years.

The ALEXI ESI is further validated against the Palmer Drought Indices (Palmer 1965, 1968), which have historically been the most commonly referenced measures of drought in the United States. Specifically, the Palmer moisture anomaly index (Z index) is the most comparable with the ALEXI stress index, which represents the departure of modeled soil moisture from the climatic mean for each month, independent of antecedent conditions.

The spatiotemporal patterns in $\Delta\overline{ESI}$ shown in Figure 9 correlate well with trends in drought conditions observed across the United States over this 3-year interval, with increasingly wet (unstressed) conditions prevailing by mid 2004. In Figure 9, the ALEXI evaporative stress anomaly index is compared with maps of the Palmer Z index. Both $\Delta\overline{ESI}$ and $\Delta\bar{Z}$ highlight the dry conditions in April 2002 that prevailed in the southwest and extended into Colorado and the southern tip of Texas. ALEXI

also picks up the drought that is beginning to develop along the East Coast. In April 2003, both indices show central Texas to be extremely dry. These hot spots persist into May, while the southeast and central Plains are classified as wetter than average. In April 2004, a band of unusually dry conditions extended from California northward into Washington State and southeastward down into Florida, as seen in both $\Delta\overline{\mathrm{ESI}}$ and $\Delta\bar{Z}$. The United States Drought Monitor for April reports that west Texas, New Mexico, and Colorado were wetter than usual because of heavy rains, which eased drought conditions in these areas, as is reflected in both indices. Overall, there is good spatial correspondence between the ALEXI and Palmer Indices, which represent two completely independent means of detecting drought conditions.

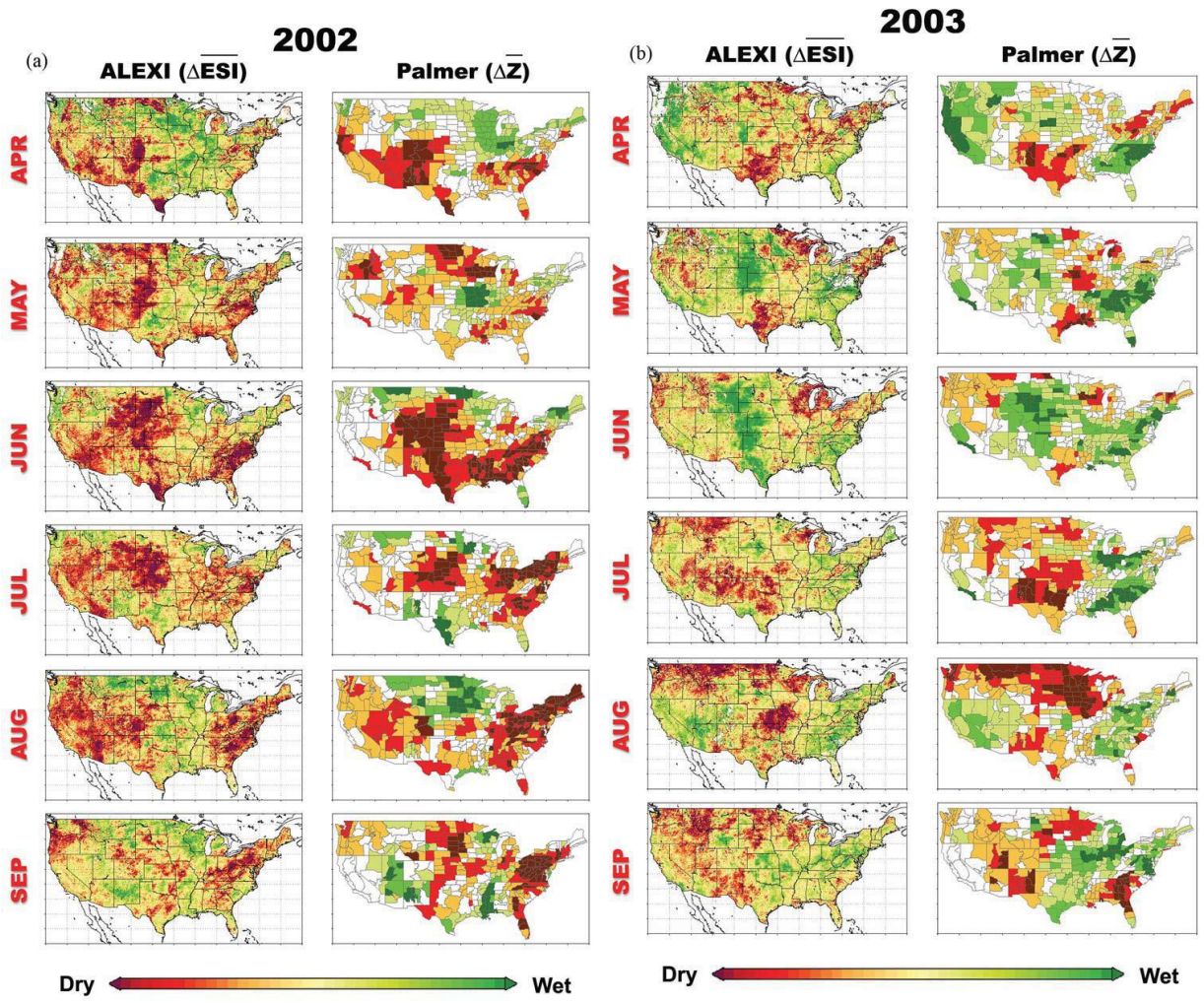
2002
(a)
ALEXI ($\Delta\overline{ESI}$)
Palmer ($\Delta\overline{Z}$)
APR
MAY
JUN
JUL
AUG
SEP
Dry
Wet
2003
(b)
ALEXI ($\Delta\overline{ESI}$)
Palmer ($\Delta\overline{Z}$)
APR
MAY
JUN
JUL
AUG
SEP
Dry
Wet

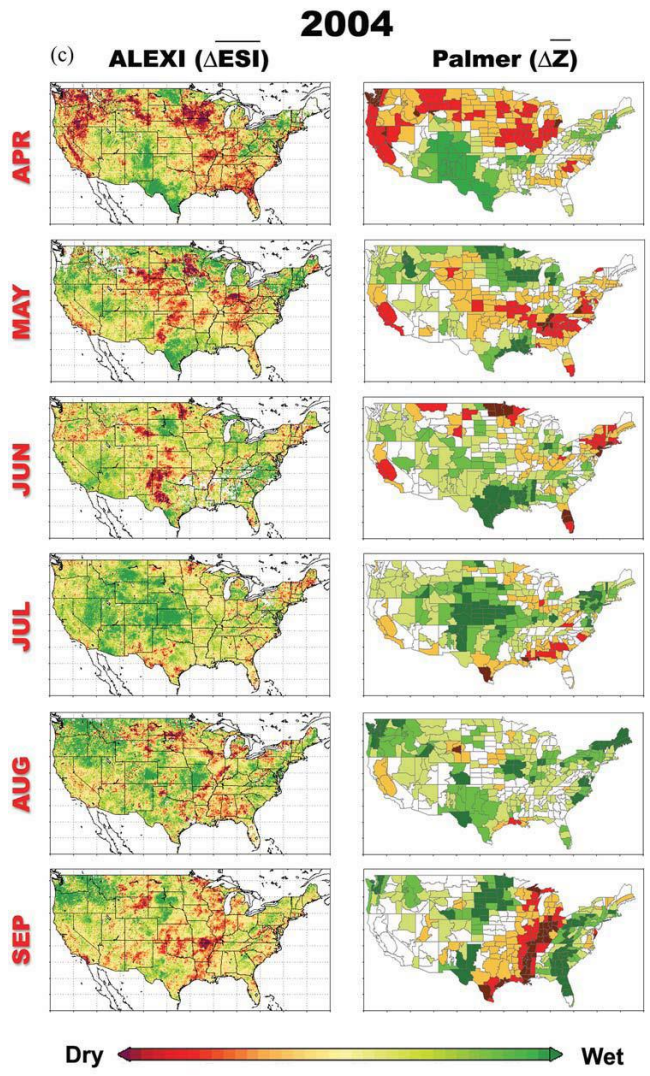

Figure 9 The 28-day clear-sky composites of the ALEX evaporative stress anomaly index, compared with anomalies in the Palmer Z index for April-September of (a) 2002, (b) 2003 and (c) 2004

3.5.3 Summary of validation

In general, the ALEXI model is able to provide accurate partitioning of sensible and latent heat fluxes across the continental United States. ALEXI ET estimates have been rigorously evaluated in comparison with ground-based data, and perform well over a range in climatic and vegetation conditions.

In addition, validation results also show that there is good qualitative agreement between spatial patterns in $\Delta\overline{ESI}$ and $\Delta\bar{Z}$, indicating a detectable impact of antecedent precipitation (as interpreted by the Palmer index) on land surface temperature at continental scales. The ALEXI evaporative stress anomaly index shows persistence in coherent spatial features from month to month, reflecting a natural time integration of moderate-term moisture conditions insofar as they affect LST and evaporative fluxes. Given its basis in remote sensing, ALEXI is able to provide stress information at significantly higher resolution than is the Palmer index.

3.6 Practical Considerations

3.6.1 Numerical Computation Considerations

The whole algorithm is composed of many straightforward calculations, thus, it is light computationally.

3.6.2 Programming and Procedural Considerations

GETD code is run every 24 hours with all the available input meteorological CFS data, GVF EVI, GOES image and IMS snow mask for the day. In the case that the any inputs data come in late, the operational procedure can be run later to make sure the missing time.

3.6.3 Quality Assessment and Diagnostics

Unit testing and system testing will include quality assessment with historical in situ observations.

3.6.4 Exception Handling

The expected exceptions, and a description of how they are identified, trapped, and handled, will be provided in a future version.

3.7 Sample Results

4. ASSUMPTIONS AND LIMITATIONS

4.1 Assumptions

It is assumed that following data are available before the ET and drought products are performed:

1. GOES thermal observations
2. Meteorological data from CFS
3. Satellite-based EVI data
4. Satellite-based snow mask data

4.2 Limitations

Major limitation of the GETD product is the input GOES data quality.
Another limitation is the area covered with snow in the winter. For the high latitude area in the North America in winter, GETD may overestimate the dry condition over snow covered area and produce low ESI values.

4.3 Potential Improvements

We are working on producing new snow mask to remove the dry values of ESI when snow is present. Another improvement is to increase the spatial resolution to 4km for the North American domain.

5. LIST OF REFERENCES

Anderson, M. C., J. M. Normal, W. P. Kustas, F. Li, J. H. Prueger & J. R. Mecikalski (2007) A climatological study of evapotranspiration and moisture stress across the continental United States: 1. Model formulation. *J. Geophys. Res.,* 112.

Anderson, M. C., J. M. Norman, G. R. Diak, W. P. Kustas & J. R. Mecikalski (1997) A two‐source time‐integrated model for estimating surface fluxes using thermal infrared remote sensing. *Remote Sens. Environ,* 60**,** 195-216.

Anderson, M. C., J. M. Norman, W. P. Kustas, F. Li, J. H. Prueger & J. R. Mecikalski (2005) Effects of vegetation clumping on two-source model estimates of surface energy fluxes from an agricultural landscape during SMACEX. *Journal of Hydrometeorology,* 6**,** 892-909.

Anderson, M. C., J. M. Norman, J. R. Mecikalski, R. D. Torn, W. P.Kustas & J. B. Basara (2004) A multi-scale remote sensing model for disaggregating regional fluxes to micrometeorological scales. *J. Hydrometeor,* 5**,** 343– 363.

Brutsaert, W. & M. Sugita (1992) Application of self-preservation in the diurnal evolution of the surface energy budget to determine daily evaporation. *J. Geophys. Res.,* 97**,** 18377–18382.

Choudhury, B. J., S. B. Idso & R. J. Reginato (1987) Analysis of an empirical model for soil heat flux under a growing wheat crop for estimating evaporation by an infrared-temperaturebased energy balance equation. *Agriculture and Forest Meteorology,* 39**,** 283–297.

Crago, R. D. (1996) Comparison of the evaporative fraction and the Priestley-Taylor a for parameterizing daytime evaporation. *Water Resources Res.,* 32**,** 1403– 1409.

Culf, A. D. (1993) The potential for estimating regional sensible heat flux from convective boundary layer growth. *Journal of Hydrology,* 146**,** 235–244.

Diak, G. R. (1990) Evaluation of heat flux, moisture flux and aerodynamic roughness at the land surface from knowledge of the PBL height and satellite-derived skin temperatures. *Agriculture and Forest Meteorology,* 52**,** 181–198.

Diak, G. R. & M. S. Whipple (1995) A note on estimating surface sensible heat fluxes using surface temperatures measured from a geostationary satellite during FIFE 1989. *Journal of Geophysical Research,* 100**,** 25453-25461.

Doran, J. C., J. M. Hubbe, J. C. Liljigren, W. J. Shaw, G. J. Collatz, D. R. Cook & R. L. Hart (1998) A technique for determining the spatial and temporal distributions of surface fluxes of heat and moisture over the Southern Great Plains Cloud and Radiation Testbed. *Journal of Geophysical Research,* 103**,** 6109–6121.

Gao, W., R. L. Coulter, B. M. Lesht, J. Qiu & M. L. Wesely (1998) Estimating clear-sky regional surface fluxes in the southern Great Plains atmospheric radiation measurement site with ground measurements and satellite observations. *Journal of Applied Meteorology,* 37**,** 5-22.

Gash, J. H. C. (1987) An analytical framework for extrapolating evaporation measurements by remote sensing surface temperatures. *International Journal of Remote Sensing,* 8**,** 1245-1249.

Gurney, R. J. & A. Y. Hsu (1990) Relating evaporative fraction to remotely sensed data at the FIFE site. *Symposium on FIFE: First ISLSCP Field Experiment, Boston, MA, February 7– 9.*

Hall, F. G., K. F. Huemmrich, S. J. Goetz, P. J. Sellers & J. E. Nickerson (1992) Satellite remote sensing of surface energy balance: Success, failures and unresolved issues in FIFE. *Journal of Geophysical Research,* 97**,** 19061-19089.

Idso, S. B., T. J. Schmugge, R. D. Jackson & R. J. Reginato (1975) The utility of surface temperature measurements for the remote sensing of surface soil water status. *Journal of Geophysical Research,* 80**,** 3044-3049.

Jackson, R. D. (1982) Soil moisture inferences from thermal-infrared measurements of vegetation temperatures. *IEEE Trans. Geosciences Remote Sensing,* 33**,** 1475–1484.

Kustas, W. P., G. R. Diak & J. M. Norman (2001) Time difference methods for monitoring regional scale heat fluxes with remote sensing. *Meteorology, and Climate: Observations and Modeling,* 3**,** 15-29.

Mason, P. J. (1988) The formation of areally-averaged roughness lengths. *Quarterly Journal of the Royal Meteorological Society,* 114**,** 399–420.

McNaughton, K. J. & T. W. Spriggs (1986) A mixed-layer model for regional evaporation *Boundary-Layer Meteorology,* 74**,** 243–262.

Mecikalski, J. M., G. R. Diak, M. C. Anderson & J. M. Norman (1999) Estimating fluxes on continental scales using remotely sensed data in an atmosphere-land exchange model. *Journal of Applied Meteorology,* 38**,** 1352-1369.

Norman, J. M. (2003) Remote sensing of surface energy fluxes at 101-m pixel resolutions. *Water Resources Research,* 39**,** 1221.

Norman, J. M., W. P. Kustas & K. S. Humes (1995) A two-source approach for estimating soil and vegetation energy fluxes from observations of directional radiometric surface temperatures. *Agricultural and Forest Meteorology,* 77**,** 263-293.

Palmer, W. C. (1965) Meteorological drought. *58 pp, U.S. Weather Bur. Res. Pap. 45, NOAA, Silver Spring, Md*.

--- (1968) Keeping track of crop moisture conditions, nationwide: The new crop moisture index. *Weatherwise,* 21**,** 156– 161.

Priestley, C. H. B. & R. J. Taylor (1972) On the assessment of surface heat flux and evaporation using large-scale parameters. *Monthly Weather Review,* 100**,** 81–92.

Shuttleworth, W. J., R. J. Gurney, A. Y. Hsu & J. P. Ormsby (1989) FIFE, the variation on energy partition at surface flux sites. *Proc. IAHS Third Int. Assembly, IAHS, Washington, D. C.*

Sugita, M. & W. Brutsaert (1991) Daily evaporation over a region from lower boundary layer profiles measured with radiosondes. *Water Resour. Res.,* 27**,** 747– 752.

Tennekes, H. (1973) A model for the dynamics of the inversion above a convective boundary layer. *Journal of Atmospheric Science,* 30**,** 558-567.

Wetzel, P. J., D. Atlas & R. Woodward (1984) Determining soil moisture from geosynchronous satellite infrared data: A feasibility study. *Journal of Climate and Applied Meteorology,* 23.

Wieringa, J. (1986) Roughness-dependent geographical interpolation of the surface wind speed averages. *Quarterly Journal of Royal Meteorological Society,* 112**,** 867–889.

Zhang, L. & R. Lemeur (1995) Evaluation of daily evapotranspiration estimates from instantaneous measurements. *Agric. For. Meteorol*, 74**,** 139– 154.

END OF DOCUMENT